Photophysical and Photocatalytic Properties of a New Series of Visible-Light-Driven Photocatalysts $M_3V_2O_8$ (M = Mg, Ni, Zn)

Defa Wang,[†,‡] Junwang Tang,[†] Zhigang Zou,[§] and Jinhua Ye*[,†,‡]

Ecomaterials Center, National Institute for Materials Science (NIMS), 1-2-1 Sengen, Tsukuba, Ibaraki 305-0047, Japan, Precursory Research for Embryonic Science and Technology (PREST), Japan Science and Technology Agency (JST), 4-1-8 Hon-cho Kawaguchi-shi, Saitama 332-0012, Japan, and Ecomaterials and Renewable Energy Research Center (ERERC), Nanjing University, 22 Hankou Road, Nanjing 210093, China

Received May 13, 2005. Revised Manuscript Received July 29, 2005

A new series of visible-light-driven photocatalysts $M_3V_2O_8$ (M = Mg, Ni, Zn) was synthesized by the conventional solid-state reaction method. The crystal structure and photophysical properties were characterized by powder X-ray diffraction and UV−vis diffuse reflectance spectroscopy, respectively. Photocatalytic properties were evaluated by O_2 evolution from an aqueous $AgNO_3$ solution under visible light irradiation. The results showed that the three compounds of $M_3V_2O_8$ (M = Mg, Ni, Zn) were all crystallized in an orthorhombic system with the space group Abam. However, the substitution of M^{2+} cations with different electronic states imposed significant effects on their photophysical and photocatalytic properties. $Zn_3V_2O_8$ showed a higher activity than $Mg_3V_2O_8$, while $Ni_3V_2O_8$ showed almost no activity. Theoretically calculated energy band structures and density of states (DOS) by the plane-wave-density function theory (DFT) revealed that the different photophysical and photocatalytic properties of $M_3V_2O_8$ (M = Mg, Ni, Zn) could be ascribed to their different electronic structures. The Zn 3d and O 2p orbitals were hybridized to construct the valence band of $Zn_3V_2O_8$, favoring the mobility of photoexcited holes in the valence band and thus promoting the O_2 evolution activity. In contrast, no such hybridization effect occurs in $Mg_3V_2O_8$ as the Mg 2p orbitals are not involved in the valence band. The split Ni 3d orbitals inserted between the O 2p and the V 3d orbitals in $Ni_3V_2O_8$ are not suitable for O_2 evolution.

Introduction

Photocatalysis using solar energy and semiconductors is of great importance in solving global energy and environment issues.[1−3] Generally, a photocatalytic reaction for water splitting involves two processes (i.e., the band gap photoexcitation to form electrons in the conduction band and holes in the valence band and, subsequently, the redox reactions on the catalyst surface to produce H_2 and O_2, respectively). The thermodynamics of redox reactions requires the conduction band bottom of a semiconductor photocatalyst to be more negative than that of the reduction potential of H_2O to form H_2 and the valence band top to be more positive than the oxidization potential of H_2O to form O_2. In view of efficient solar energy conversion, it is necessary to develop visible-light-driven photocatalysts since visible light accounts for ∼43% of whole solar energy while UV light occupies merely ∼4%. Particularly, in constructing a Z-scheme photoelectrochemical system (PEC) for water splitting,[4] the photocatalysts able to evolve O_2 and H_2 are both indispensable.

So far, however, the number of visible-light-driven photocatalysts for H_2/O_2 evolution is still limited even if the redox reaction is assisted with an electron donor (e.g., CH_3OH) or an electron scavenger (e.g., $AgNO_3$). Essentially, a visible-light-driven semiconductor material capable of photocatalytic water splitting should have a small band gap able to absorb visible light and appropriate band edges suitable for the redox reactions of H_2 and O_2 evolution. One of the strategies employed for the development of visible-light-driven oxide semiconductor photocatalysts is to introduce foreign elements (usually the 3d transition metals) into an active photocatalyst with a wide band gap to form a separate donor level in the forbidden band. For example, photocatalytic H_2 evolution has been reported over Cr doped TiO_2 and $SrTiO_3$,[5−10] Sb/Nb/Ta and Cr co-doped $SrTiO_3$[11] under visible light irradiation. Another effective method is to lift the valence band top to a more negative position than O 2p and/or lower the conduction band bottom to a more positive position.[12] Since the V 3d band is usually located below the

* Corresponding author. Fax: +81-298-59-2601. E-mail: jinhua.ye@nims.go.jp.
† National Institute for Materials Science.
‡ Japan Science and Technology Agency.
§ Nanjing University.

(1) Fujishima, A.; Honda, K. *Nature* **1972**, *238*, 37.
(2) Hoffman, M. R.; Martin, S. T.; Choi, W.; Bahnemann, D. W. *Chem. Rev.* **1995**, *95*, 69.
(3) Zou, Z.; Ye, J.; Sayama, K.; Arakawa, H. *Nature* **2001**, *414*, 625.
(4) Sayama, K.; Yoshida, R.; Kusama, H.; Okabe, K.; Abe, Y.; Arakawa, H. *Chem. Phys. Lett.* **1997**, *277*, 387.
(5) Herrmann, J.-M.; Disdier, J.; Pichat, P. *Chem. Phys. Lett.* **1984**, *106*, 618.
(6) Borgarello, E.; Kiwi, J.; Grantzel, M.; Pelizetti, E.; Visca, M. *J. Am. Chem. Soc.* **1982**, *104*, 2996.
(7) Karakitsou, K. E.; Verykios, X. E. *J. Phys. Chem.* **1993**, *97*, 1184.
(8) Mu, W.; Herrmann, J.-M.; Pichat, P. *Catal. Lett.* **1989**, *3*, 73.
(9) Choi, W.; Termin, A.; Hoffmann, M. R. *J. Phys. Chem.* **1994**, *98*, 13669.
(10) Umebayashi, T.; Yamaki, T.; Itoh, H.; Asai, K. *J. Phys. Chem. Solids* **2002**, *63*, 1909.
(11) Kato, H.; Kudo, A. *J. Phys. Chem. B* **2002**, *106*, 5029.

10.1021/cm051016x CCC: $30.25
Published on Web 09/09/2005

analogous d bands of the other transition metals in the energy spectrum,[13] some vanadium-containing oxides such as $BiVO_4$[14,15] with a deformed scheelite structure and $InVO_4$[16] composed of VO_4 tetrahedra and InO_6 octahedra have been developed successfully as visible-light-driven photocatalysts for O_2 or H_2 evolution in the presence of sacrificial reagents $AgNO_3$ or CH_3OH, respectively.

In a previous study of the photocatalysts $M_{2.5}VMoO_8$ (M = Mg, Zn) crystallized in the orthorhombic system with the space group *Pnma* for M = Mg and $P2_12_12_1$ for M = Zn, respectively, we have found that the two photocatalysts show quite different activities for O_2 evolution due to the substitution of M^{2+} cations.[17] In this paper, we report a new series of photocatalysts $M_3V_2O_8$ (M = Mg, Ni, Zn) crystallized in an orthorhombic system with the same space group Abam. The substitution effects of the divalent cations M^{2+} on the electronic structure and photophysical and photocatalytic properties of $M_3V_2O_8$ (M = Mg, Ni, Zn) are studied. The energy band structures and density of states (DOS) are calculated by the plane-wave-density function theory (DFT). On the basis of experimental and theoretical results, the correlation between photocatalytic activity and electronic structure is discussed.

Experimental Procedures

Synthesis and Characterization of Photocatalysts. Polycrystalline $M_3V_2O_8$ (M = Mg, Ni, Zn) powder samples were prepared by the conventional solid-state reaction method. Reagent grade oxides MgO, NiO, ZnO, and V_2O_5 (Wako, purity: 99.99%) were mixed in the stoichiometric proportion of $M_3V_2O_8$ (M = Mg, Ni, Zn), milled carefully with the addition of ethanol, and then preliminarily calcined at 600 °C in an alumina crucible in air for 20 h. After pelletizing, the samples were finally calcined at 1000 °C for $Mg_3V_2O_8$, 750 °C for $Ni_3V_2O_8$, and 780 °C for $Zn_3V_2O_8$, respectively, for 40 h with one intermittent grinding. Equilibrium was confirmed as no further change in the X-ray diffraction (XRD) patterns was detected. The XRD pattern was measured on an X-ray diffractometer (JEOL JDX-3500, Japan) with Cu Kα radiation (λ = 1.54178 Å). The UV−vis diffuse reflectance spectrum was measured using a UV−vis spectrometer (UV-2500, Shimadzu, Japan) at room temperature and was converted to an absorbance spectrum by the Kubelka−Munk method. A scanning electron microscope (SEM, JEOL JSM-6500F, Japan) equipped with an X-ray energy dispersive spectrometer (EDS) was employed for morphology observation and composition analysis. The surface area was measured on a Gemini-2360 analyzer (Micromeritics, Shimadzu, Japan) by nitrogen absorption at 77 K using the Brunauer−Emmett−Teller (BET) method.

Evaluation of Photocatalytic Activity. Photocatalytic reactions were carried out in an outer irradiation Pyrex glass cell connected to a closed gas circulation system. The light source was a 300 W xenon arc lamp (ILC Technology, CERMAX LX-300, operated at 200 W), which was focused on the side window of the reaction cell through a long-pass cutoff filter ($\lambda \geq 420$ nm; L42, HOYA). For O_2 evolution, the catalyst powders (0.5 g) were dispersed by a magnetic stirrer in an aqueous $AgNO_3$ solution (5 mM of $AgNO_3$ + 270 mL of H_2O) in the reaction cell. $AgNO_3$ was used as an electron acceptor. Before reaction, the closed gas circulation system and the reaction cell were well-evacuated and then introduced into ~2.5 kPa argon gas. Upon irradiation, the oxygen gas evolved was mixed with argon gas by a glass piston pump and was in situ analyzed with an online TCD gas chromatograph (Shimadzu GC-8AIT, argon carrier). The photon efficiency or quantum yield (QY) of O_2 evolution at λ = 420.4 nm was measured by using an interference band-pass filter (λ_0 = 420.4 nm, T_{max} = 44.8%, $\Delta\lambda/2$ = 14.7 nm, Kenko). A thermopile was used for measuring the intensity of incident light and then transferred to the number of incident photons. The apparent quantum yield (%) of O_2 was calculated by the following equation: QY (%) = $N_h/N_p = 4N_{O2}/N_p$, where N_h is the number of reacted holes, N_{O2} is the number of O_2 molecules evolved, and N_p is the number of incident photons.

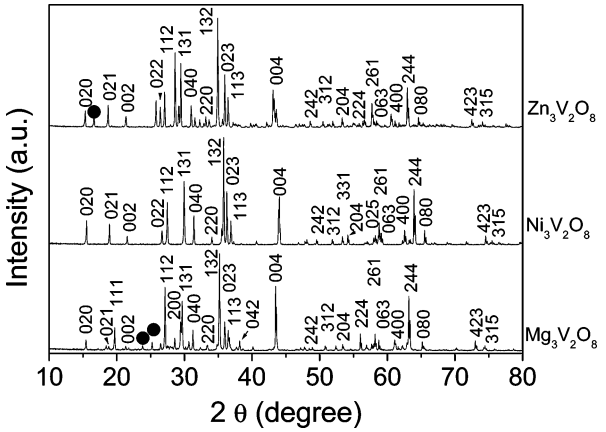

Figure 1. X-ray diffraction patterns of the as-synthesized $M_3V_2O_8$ (M = Mg, Ni, Zn) powder samples at room temperature. Except for a few impurities (●), all peaks could be indexed according to the JCPDS card no. 37-0351 for M = Mg, no. 70-1394 for M = Ni, and no. 34-0378 for M = Zn, respectively.

Calculation Method of Band Structure. The plane-wave-density function (DFT) calculation was performed using the CASTEP program (Materials Studio, Accelrys Inc.).[18] The core electrons were replaced with ultrasoft pseudo-potentials. The generalized gradient approximation (GGA-RPBE) was applied. The kinetic energy cutoff was selected as 260 eV for all calculations.

Results and Discussion

Crystal Structure. Figure 1 shows the XRD patterns of the $M_3V_2O_8$ (M = Mg, Ni, Zn) powder samples at room temperature and the indexed results according to the JCPDS card no. 37-0351 for M = Mg, no. 70-1394 for M = Ni, and no. 34-0378 for M = Zn, respectively. Except for little amounts of impurity phases (ca. < 5%), the samples were crystallized in an orthorhombic system with the space group Abam. By the least-squares refinement method, the crystal lattice parameters were calculated as follows: a = 8.329(5) Å, b = 11.453(5) Å, and c = 6.071(3) Å for $Mg_3V_2O_8$; a = 8.241(3), b = 11.411(10), and c = 5.941(2) for $Ni_3V_2O_8$; and a = 8.306(1) Å, b = 11.540(1) Å, and c = 6.117(1) Å for $Zn_3V_2O_8$. Basically, the variation of lattice constants was dependent on the ionic radii of the M^{2+} cations (Mg^{2+}: 0.72

(12) Tsuji, I.; Kato, H.; Kobayashi, H.; Kudo, A. *J. Am. Chem. Soc.* **2004**, *126*, 13406.
(13) Oshikiri, M.; Boero, M.; Ye, J.; Zou, Z.; Kido, G. *J. Chem. Phys.* **2002**, *117*, 7313.
(14) Kudo, A.; Ueda, K.; Kato, H.; Mikami, I. *Catal. Lett.* **1998**, *53*, 229.
(15) Kudo, A.; Omori, K.; Kato, H. *J. Am. Chem. Soc.* **1999**, *121*, 11459.
(16) Ye, J.; Zou, Z.; Oshikiri, M.; Matsushita, A.; Shimoda, M.; Imai, M.; Shishido, T. *Chem. Phys. Lett.* **2002**, *356*, 221.
(17) Wang, D.; Zou, Z.; Ye, J. *Catal. Today* **2004**, *93*−*95*, 885.
(18) Payne, M. C.; Teter, M. P.; Allan, D. C.; Arias, T. A.; Joannopoulos, J. D. *Rev. Mod. Phys.* **1992**, *64*, 1045.

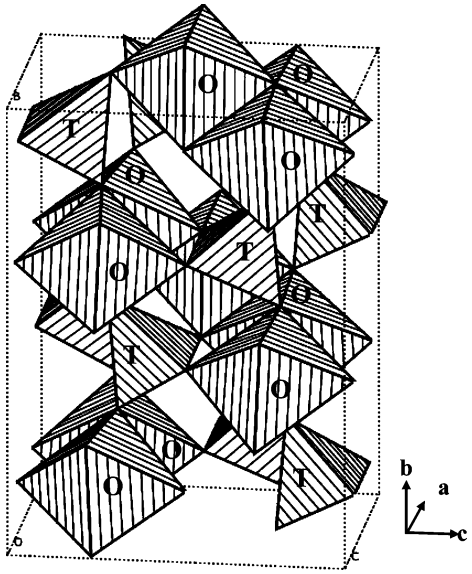

Figure 2. Orthorhombic structure of $M_3V_2O_8$ is composed of the VO_4 tetrahedra (T) and the MO_6 octahedra (O) (M = Mg, Ni, Zn). Space group: Abam.

Å; Ni^{2+}: 0.69 Å; and Zn^{2+}: 0.74 Å).[19] These results were consistent with those reported previously.[20−23] As shown in Figure 2, the crystal structure of $M_3V_2O_8$ is composed of the VO_4 tetrahedra and the MO_6 octahedra (M = Mg, Ni, Zn). We suppose that the cations M^{2+} (M = Mg, Ni, Zn) in the octahedral field with different electronic states should impose significant effects on the electronic structure and photophysical and photocatalytic properties of the studied compounds.

The morphologies of the $M_3V_2O_8$ (M = Mg, Ni, Zn) powder samples were observed with SEM, and the compositions were analyzed with EDS equipped with the SEM. It confirmed that the overall compositions were in agreement with those of the as-designed compounds and that the elements were distributed homogeneously. The BET surface areas were measured to be ∼0.6 m^2/g for $Mg_3V_2O_8$, ∼0.8 m^2/g for $Ni_3V_2O_8$, and ∼0.5 m^2/g for $Zn_3V_2O_8$, respectively, which were consistent with the particle sizes as observed by SEM. The samples, after the aforementioned photocatalytic reactions, were checked again with XRD and EDS. Except for the photoreduced metallic silver from $AgNO_3$ on the catalyst surface, no changes in both crystal structure and surface compositions were detected, indicating the stability of the photocatalysts against light irradiation.

UV−vis Diffuse Reflectance Spectra. Figure 3 shows the UV−vis diffuse reflectance spectra of the $M_3V_2O_8$ (M = Mg, Ni, Zn) powder samples at room temperature. The main absorption edges were ∼410 nm (e_g: ∼3.02 eV) for M = Mg, ∼550 nm (e_g: ∼2.25 eV) for M = Ni, and ∼425 nm (e_g: ∼2.92 eV) for M = Zn, respectively. In general, all

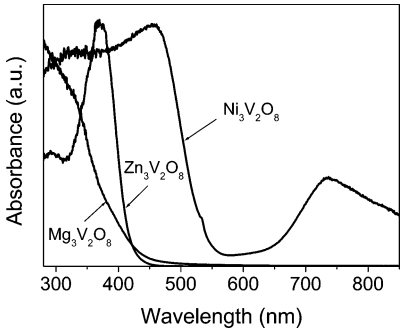

Figure 3. UV−vis diffuse reflectance spectra of the $M_3V_2O_8$ (M = Mg, Ni, Zn) powder samples at room temperature.

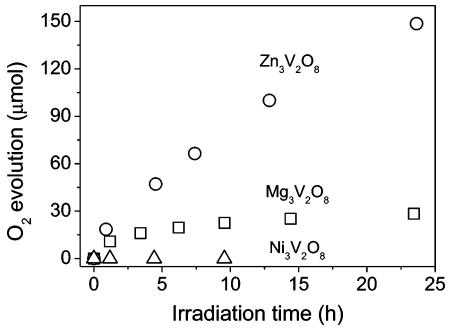

Figure 4. Photocatalytic O_2 evolution from aqueous $AgNO_3$ (5 mmol) solution suspended with $M_3V_2O_8$ (M = Mg, Ni, Zn) powder catalysts (0.5 g) under visible light irradiation ($\lambda \geq 420$ nm).

compounds hold the band gaps that are able to absorb visible light, implying the possibility of photocatalytic activity over these materials under visible light irradiation. The prolonged absorption tail until ∼510 nm in the spectrum of $Mg_3V_2O_8$ should result from the crystal defects formed at an elevated calcination temperature for $Mg_3V_2O_8$ in comparison with the other two compounds. The spectrum of $Ni_3V_2O_8$ shows that the main absorption edge has been shifted to ∼550 nm, indicating that the substitution of Ni^{2+} significantly reduced the band gap. In addition, an apparent absorption hump with an extrapolated absorption edge at ∼950 nm (∼1.3 eV) was observed. Preliminarily, this additional absorption could be ascribed to the d−d electron transition between the split Ni 3d orbitals in the octahedral field.[24] Further details will be discussed in combination with the calculated electronic structures in the following section.

Photocatalytic Activities. The activities of O_2 evolution from an aqueous $AgNO_3$ (5 mmol) solution over the $M_3V_2O_8$ (M = Mg, Ni, Zn) powder catalysts (0.5 g) under visible light irradiation ($\lambda \geq 420$ nm) are shown in Figure 4. In the initial 5 h of reaction, the average evolution rates were 10.2 μmol/h for $Zn_3V_2O_8$, 3.6 μmol/h for $Mg_3V_2O_8$, and 0.0 μmol/h for $Ni_3V_2O_8$ respectively. Using an interference bandpass filter ($\lambda_0 = 420.4$ nm, $T_{max} = 44.8\%$, and $\Delta\lambda/2 = 14.7$ nm), the average quantum yields (QY) at $\lambda = 420.4$ nm in the initial 5 h of reaction were measured to be ∼0.64% for $Zn_3V_2O_8$ and ∼0.23% for $Mg_3V_2O_8$, respectively, which were in agreement with the average evolution rates. Generally speaking, the activity of a photocatalyst increases with an increase in surface area because the photocatalytic reaction usually takes place on the catalyst surface. As shown in Table

(19) Shannon, R. D. *Acta Crystallogr., Sect. A* **1976**, *A32*, 751.
(20) Harding, W. D.; Kung, H. H.; Kozhevnikov, V. L.; Poeppelmeier, K. R. *J. Catal.* **1993**, *144*, 593.
(21) Wang, X.; Stern, C. L.; Poeppelmeier, K. R. *J. Alloys Compd.* **1996**, *243*, 51.
(22) Fuess, H.; Bertaut, E. F.; Pauthenent, R.; Durif, A. *Acta Crystallogr., Sect. B* **1970**, *B26*, 2036.
(23) Sauerbrei, E. E.; Faggiani, R.; Calvo, C. *Acta Crystallogr., Sect. B* **1973**, *B29*, 2304.
(24) Serpone, N.; Lawless, D. *Langmuir* **1994**, *10*, 643.

Table 1. Crystal Structures, Lattice Parameters, Photophysical Properties, and Photocatalytic Activities of $M_3V_2O_8$ (M = Mg, Ni, Zn)

photocatalysts	crystal structure	space group	lattice parameters (Å)	band gap (eV)	surface area (m^2/g)	O_2 evolution rate (μmol/h)	quantum yield (%)
$Mg_3V_2O_8$	orthorhombic	Abam	$a = 8.329(5)$, $b = 11.453(5)$, $c = 6.071(3)$	3.02	0.6	3.6	0.23
$Ni_3V_2O_8$	orthorhombic	Abam	$a = 8.241(3)$, $b = 11.411(10)$, $c = 5.941(2)$	2.25	0.8	0	0
$Zn_3V_2O_8$	orthorhombic	Abam	$a = 8.306(1)$, $b = 11.540(1)$, $c = 6.117(1)$	2.92	0.5	10.2	0.64

1, the surface areas of $Mg_3V_2O_8$ and $Zn_3V_2O_8$ are very close. Therefore, we may conclude that the O_2 evolution rate of $Zn_3V_2O_8$ is intrinsically higher than that of $Mg_3V_2O_8$. In this sense, it is expected that the activities of the present photocatalysts can be improved significantly if the materials are synthesized by means of chemical methods (e.g., sol−gel) so as to obtain large surface areas.

A dark test with $Zn_3V_2O_8$ showed that no O_2 was evolved when the irradiation light was turned off. The wavelength dependence of O_2 evolution performed with $Zn_3V_2O_8$ using a series of cutoff filters is shown in Figure 5. It is consistent with the UV−vis diffuse reflectance spectrum. All these results confirmed that the O_2 evolution was inherently the result of a photocatalytic reaction. It should be pointed out that the gradual decrease of O_2 evolution rate with increase of irradiation time was probably due to the shielding effect by more and more metallic silver reduced on the catalyst surface from the $AgNO_3$ solution during photocatalytic reactions.[15]

Photocatalytic H_2 evolution from aqueous methanol solution was also performed over the Pt (0.2 wt %)/$M_3V_2O_8$ (M = Mg, Ni, Zn) powder samples. The experimental conditions for H_2 evolution have been described elsewhere.[25] No H_2 evolution was obtained over any studied photocatalysts under both UV and visible light irradiations. It implies that the potential levels of the conduction band bottoms might not be suitable for H_2 evolution. The aforementioned photophysical and photocatalytic properties will be discussed in connection with the theoretically calculated energy band structures.

Energy Band Structures. The previously mentioned experimental results are summarized in Table 1. We can see that, although $M_3V_2O_8$ (M = Mg, Ni, Zn) have the same crystal structure, their photocatalytic activities of O_2 evolution are quite different. It is well-known that, in addition to the crystal structure, the electronic structure of a semiconductor material usually plays a dominant role in its functional properties such as photocatalytic activity. With the crystal data as summarized in Table 1 and the atomic coordinates and occupation factors,[20−23] the electronic structures of $M_3V_2O_8$ (M = Mg, Ni, Zn) were calculated by the plane-wave-density function theory (DFT) using the CASTEP program package. Figure 6a,a′,b,b′,c,c′ shows the calculated band structures and projected total density of states (DOS) for $Mg_3V_2O_8$, $Ni_3V_2O_8$, and $Zn_3V_2O_8$, respectively. We can see that the conduction bands (CBs) of all three compounds are primarily comprised of the empty V 3d orbitals (the t_2 state in a tetrahedral field) and some contributions from the empty Ni 3d or Zn 4s orbitals with respect to the type of M^{2+} cations. For $Zn_3V_2O_8$, the involvement of the empty Zn 4s orbitals reduces the CB bottom of $Zn_3V_2O_8$ to a lower potential level than that of $Mg_3V_2O_8$. This is probably one of the reasons that the band gap of $Zn_3V_2O_8$ is smaller than that of $Mg_3V_2O_8$. For the case of $Ni_3V_2O_8$, the split Ni 3d orbitals—the occupied (t_{2g} + b_{1g}) states and the empty b_{2g} state—in the octahedral crystal field are supposed to play an important role in determining the electronic structure.[26] From Figure 6b,b′, we can see that the CB bottom of $Ni_3V_2O_8$ determined by the empty Ni 3d orbitals is much lower than those of not only $Mg_3V_2O_8$ but also $Zn_3V_2O_8$. As mentioned previously, the CB bottoms of all the three compounds are suggested to be located below the potential level for H_2 evolution because no H_2 could be evolved over Pt (0.2 wt %)/$M_3V_2O_8$ under either UV or visible light irradiation. It should be pointed out that the CB bottom of $Ni_3V_2O_8$ might even be lower than that for reducing the sacrificial reagent Ag^+ ($AgNO_3$) to Ag by the photoinduced electrons, and simultaneously, the process for oxidating H_2O to evolve O_2 by the photoinduced holes is suppressed. As a result, $Ni_3V_2O_8$ shows no activity for O_2 evolution, although the potential level of O 2p orbitals is positive sufficiently. According to the ligand field theory (LFT),[27] the split energy of 3d orbitals in a tetrahedral crystal field is usually about half of that in an octahedral crystal field for a given transition metal, so the higher energy state of the split 3d orbitals in a tetrahedral crystal field usually lies at a lower potential level. This is probably the crucial reason that the $M_3V_2O_8$ (M = Mg, Ni, Zn) containing VO_4 tetrahedra are not able to evolve H_2 even under UV light irradiation.

The valence band (VB) structures of $M_3V_2O_8$ are quite different. The VB of $Mg_3V_2O_8$ is mainly composed of O 2p and the occupied V 3d orbitals (the e state in a tetrahedral field), whereas the VB of $Zn_3V_2O_8$ is composed of not only O 2p and the occupied V 3d orbitals (the e state) but also the fully filled Zn 3d orbital. As Zn 3d is below O 2p, their hybridization does not shift the VB top upward so much and thus has almost no contribution to narrowing the band gap of $Zn_3V_2O_8$. Nevertheless, the hybridization of Zn 3d and O

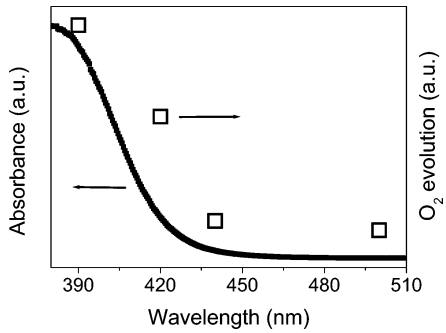

Figure 5. Wavelength dependence of O_2 evolution from aqueous $AgNO_3$ (5 mmol) solution suspended with the $Zn_3V_2O_8$ powder catalyst (0.5 g), showing good consistency with the absorption spectrum. Reaction time: 5 h.

(25) Wang, D.; Zou, Z.; Ye, J. *Chem. Mater.* **2005**, *17*, 3255.
(26) Wang, D.; Zou, Z.; Ye, J. *Chem. Phys. Lett.* **2005**, *411*, 285.
(27) Schriver, D. F.; Atkins, P.; Langford, C. H. *Inorganic Chemistry*, 2nd ed.; W. H. Freeman: New York, 1994.

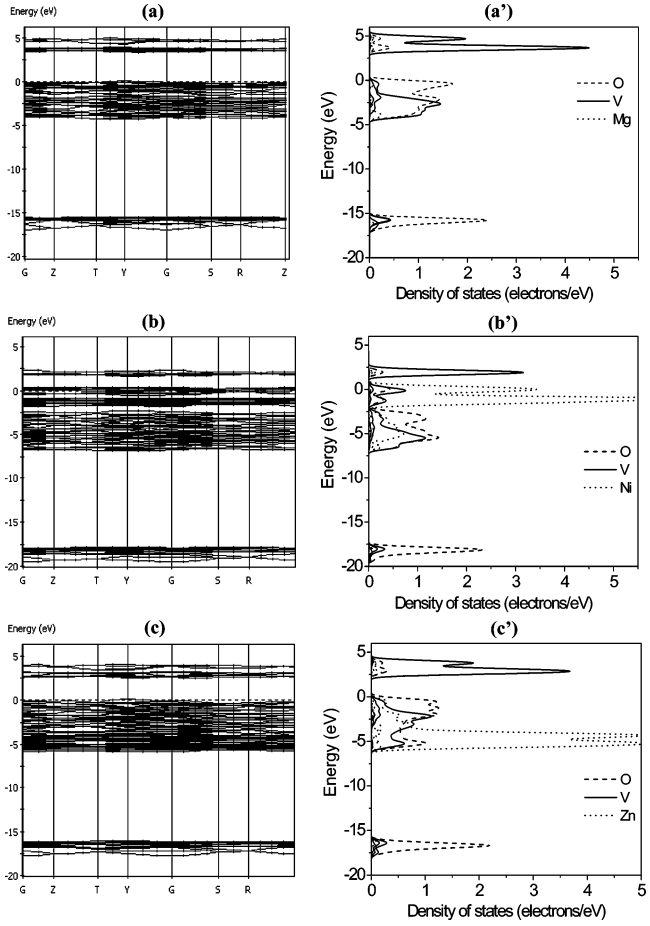

Figure 6. Band structures and projected total density of states (DOS) for (a and a′) $Mg_3V_2O_8$, (b and b′) $Ni_3V_2O_8$, and (c and c′) $Zn_3V_2O_8$. The potential level of the Mg 2p orbitals is about −40 eV, which is not shown in the figure. See text for details.

2p orbitals increases the density of states as well as the width of valence band. As a consequence, the mobility of photoinduced holes and hence the O_2 evolution activity for $Zn_3V_2O_8$ is promoted in comparison with that for $Mg_3V_2O_8$, of which the VB is mainly composed of the more localized O 2p orbitals. For $Ni_3V_2O_8$, the occupied Ni 3d ($t_{2g} + b_{1g}$) orbitals in the octahedral field are located at a more negative position above O 2p. The excitation of photoinduced electrons from O 2p to the empty Ni 3d b_{2g} orbitals accounts for the main absorption at ∼550 nm (∼2.25 eV), whereas the transition from the occupied Ni 3d ($t_{2g} + b_{1g}$) orbitals to the empty Ni 3d b_{2g} orbitals is supposed to correspond to the additional absorption hump with an extrapolated absorption edge at ∼950 nm (∼1.3 eV) (see Figure 3). Thermodynamically, the potential levels of both the O 2p and the occupied Ni 3d ($t_{2g} + b_{1g}$) orbitals might be positive enough for oxidation of water to form O_2. In practice, however, no O_2 evolution was observed over $Ni_3V_2O_8$. As mentioned previously, the most important reason is that the CB bottom of $Ni_3V_2O_8$ determined by the empty Ni 3d b_{2g} orbitals is too low to reduce the sacrificial reagent Ag^+ ($AgNO_3$) to Ag by the photoinduced electrons. The other reason is the kinetic limitation (i.e., the reaction for evolving one molecule O_2 usually involves a four-hole oxidation of water,[28] which

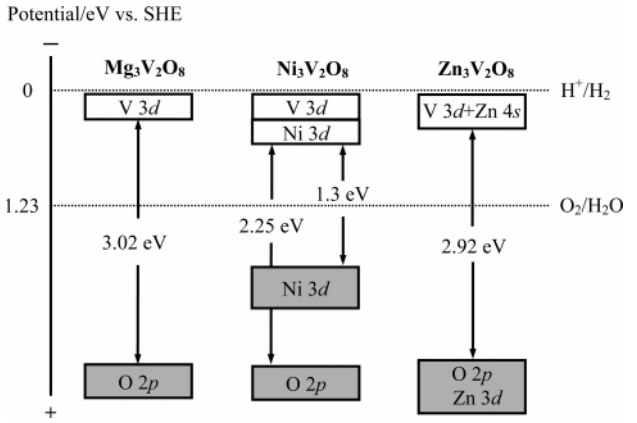

Figure 7. Schematic band structures of $M_3V_2O_8$ (M = Mg, Ni, Zn). The Zn 3d and O 2p orbitals are hybridized to form the VB of $Zn_3V_2O_8$. The Mg 2p is located far below the O 2p orbitals, without contribution to the VB of $Mg_3V_2O_8$. The split Ni 3d orbitals are inserted between O 2p and the empty V 3d orbitals of $Ni_3V_2O_8$, over which no O_2 is able to evolve. The CBs are mainly composed of the empty V 3d orbitals and some contribution from Ni 3d or Zn 4s orbitals with respect to the type of M^{2+} cations. The CB bottom levels are more positive than the potential level of H_2 evolution.

requires a relatively large overpotential). The calculated band gaps of $M_3V_2O_8$ are in the order of $Mg_3V_2O_8$ > $Zn_3V_2O_8$ > $Ni_3V_2O_8$, being consistent with those estimated from the UV−vis diffuse reflectance spectra as shown in Figure 3. As the Zn 3d and Ni 3d orbitals are strongly hybridized with the O 2p orbitals, we can deduce that the Zn−O and Ni−O bonds are mainly covalent in the ZnO_6 and NiO_6 octahedra. On the contrary, the Mg 2p orbitals lie far below the O 2p orbitals (c.a. −40 eV, not shown in Figure 6a,a′) and have no contribution to the valence band. It indicates that the Mg−O bond is mainly ionic in the MgO_6 octahedron. The different bond properties of Mg−O, Ni−O, and Zn−O can be attributed to their different electronegativities. On the basis of the experimental and theoretically calculated results, the energy band structures of $M_3V_2O_8$ (M = Mg, Ni, Zn) are proposed and schematically illustrated in Figure 7.

As mentioned previously, the substitution of M^{2+} cations with different electronic states (Mg^{2+}: $2p^6$; Ni^{2+}: $3d^8$; and Zn^{2+}: $3d^{10}$) in the octahedral field significantly influences the electronic structures and thus the photophysical and photocatalytic properties of $M_3V_2O_8$ (M = Mg, Ni, Zn). The role of d electron states in defining the electronic properties of several II−VI semiconductors has been extensively discussed by Wei and Zunger.[29] They have concluded that the p−d hybridization lifts the top edge of the valence band upward without affecting the bottom edge of the conduction band. Sampath et al.[30] have studied the electronic structure of $ZnGa_2O_4$ by means of the self-consistent tight-binding linearized muffin-tin orbital method with the atomic sphere approximation. It also shows that the hybridization of Zn 3d with the O 2p orbitals shifts the valence band edge upward. Recently, Kato et al. have reported a water splitting photocatalyst $AgMO_3$ (M = Nb, Ta), in which the Ag 4d and O 2p orbitals are hybridized to form the valence band at a more negative level than O 2p.[31]

(28) Konta, R.; Ishii, T.; Kato, H.; Kudo, A. *J. Phys. Chem. B* **2004**, *108*, 8992.
(29) Wei, S. H.; Zunger, A. *Phys. Rev.* **1988**, *B37*, 8958.
(30) Sampath, S. K.; Kanhere, D. G.; Pandey, R. J. *J. Phys.: Condens. Matter* **1999**, *11*, 3635.

The present study and those reported previously[29−31] demonstrate that, depending on the crystal structure, the p−d orbital hybridization between O^{2-} and the metal ions (e.g., Zn^{2+} and Ag^{+}) with the d^{10} configuration plays versatile roles in, for instance, narrowing of the band gap, shifting of the band edges, or broadening of the bandwidth. Apparently, the different photocatalytic activities of O_2 evolution are closely related to the different electronic structures of $M_3V_2O_8$ (M = Mg, Ni, Zn).

Conclusions

The $M_3V_2O_8$ (M = Mg, Ni, Zn) compounds crystallized in an orthorhombic system with the space group of Abam have been found to be a novel series of visible-light-driven photocatalysts for O_2 evolution. The M^{2+} cations with different electron states play a significant role in the electronic structures and photophysical and photocatalytic properties of $M_3V_2O_8$ (M = Mg, Ni, Zn). The energy band structures theoretically calculated by the plane-wave-density function theory (DFT) show that the Zn 3d and O 2p orbitals are hybridized to construct the valence band of $Zn_3V_2O_8$, whereas the Mg 2p orbitals are not involved in the valence band of $Mg_3V_2O_8$. For $Ni_3V_2O_8$, the split Ni 3d orbitals are inserted between O 2p and V 3d orbitals. The hybridization of Zn 3d with O 2p orbitals favors the mobility of photoexcited holes in the valence band and thus promotes the O_2 evolution activity for $Zn_3V_2O_8$. The present study suggests that the p−d hybridization effect (e.g, O 2p and Zn 3d) can be utilized by incorporating metal cations (e.g., Zn^{2+}) with the d^{10} configuration in designing oxide semiconductors with improved photocatalytic activities.

CM051016X

(31) Kato, H.; Kobayashi, H.; Kudo, A. *J. Phys. Chem. B* **2002**, *106*, 12441.